

Electronic Supplementary Information

Antibacterial Activity of Copper Pyrazolate Coordination Polymers

Corrado Di Nicola,^{*a} Fabio Marchetti,^a Alessia Tombesi,^b Sonila Xhafa,^a Patrizio Campitelli,^a Marco Moroni,^{c,d} Simona Galli,^{c,e} Riccardo Pettinari,^b Claudio Pettinari^b

^a ChIP Research Center, School of Science and Technology, University of Camerino, via Madonna delle Carceri, 62032 Camerino MC, Italy.

^b ChIP Research Center, School of Pharmacy, University of Camerino, via Madonna delle Carceri, 62032 Camerino MC, Italy.

^c Dipartimento di Scienza e Alta Tecnologia, Università degli Studi dell'Insubria, Via Valleggio 9, 22100 Como, Italy.

^d Dipartimento di Chimica, Università degli Studi di Pavia, Via Taramelli 16, 27100 Pavia, Italy.

^e Consorzio Interuniversitario Nazionale per la Scienza e Tecnologia dei Materiali, Via Giusti 9, 50121 Firenze, Italy.

Index:

- Figure S1.** IR spectra of **2** (blue) and **5** (black). Pag. S2
- Figure S2.** TGA curves of **2** (blue), **5** (black) and **5** after thermal treatment at 433 K for 1 h (red). Pag. S2
- Figure S3.** IR spectra of **2** (blue) and **5** after heating at 433 K for 1h (orange). The two spectra are superimposable, confirming the transformation of **5** in **2** after the thermal treatment. Pag. S3
- Figure S4.** Graphical result of the final structure refinement carried out with the Rietveld method on the PXRD pattern of **2** in terms of experimental, calculated and difference traces (blue, red and grey, respectively). The green markers at the bottom indicate the positions of the Bragg reflections. Pag. S3
- Figure S5.** Graphical result of the whole powder pattern refinement carried out with the Le Bail approach on the PXRD pattern of **5** in terms of experimental, calculated and difference traces (blue, red and grey, respectively). The green markers at the bottom indicate the positions of the Bragg reflections. Pag. S4
- Figure S6.** Antibacterial activity of the pyrazole ligands against *E. coli* (up), *S. aureus* (down) Pag. S5

Supporting Information

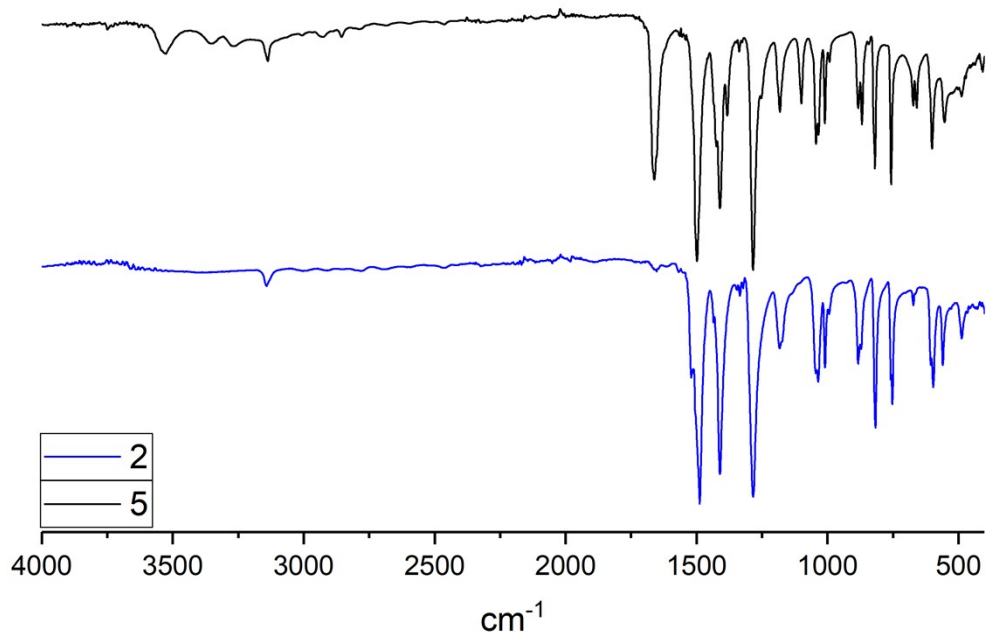


Figure S1. IR spectra of **2** (blue) and **5** (black).

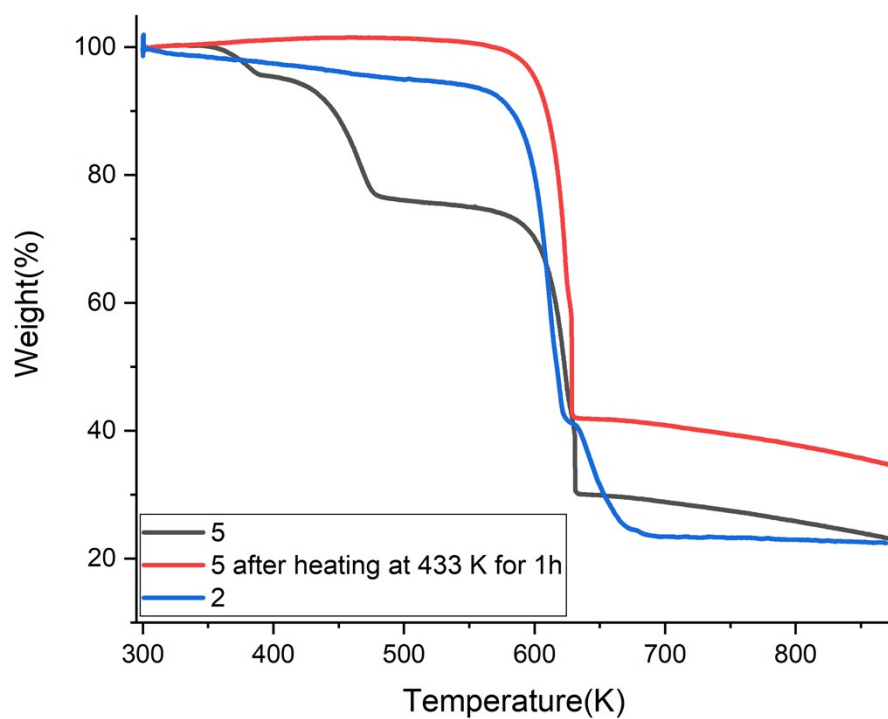


Figure S2. TGA curves of **2** (blue), **5** (black) and **5** after thermal treatment at 433 K for 1 h (red).

Supporting Information

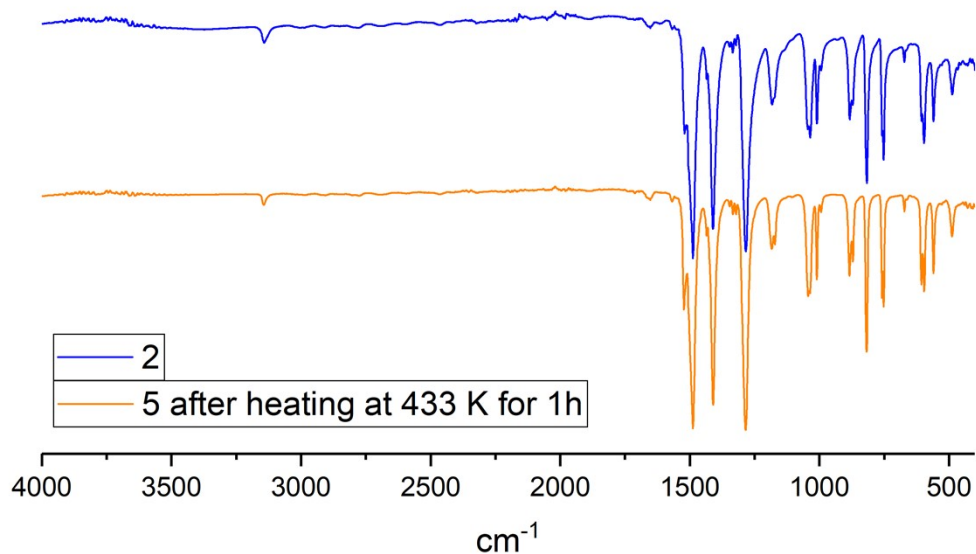


Figure S3. IR spectra of **2** (blue) and **5** after heating at 433 K for 1h (orange). The two spectra are superimposable, confirming the transformation of **5** in **2** after the thermal treatment.

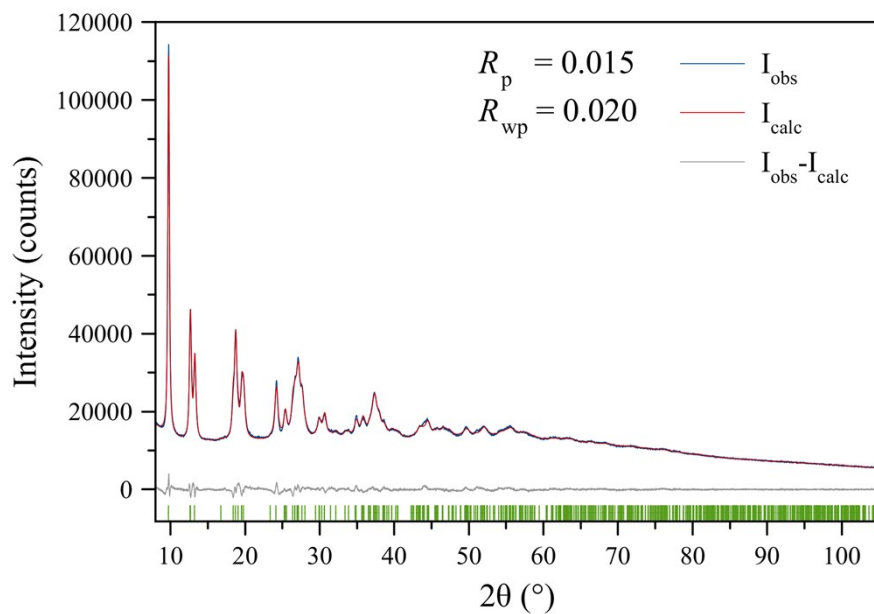


Figure S4. Graphical result of the final structure refinement carried out with the Rietveld method on the PXRD pattern of **2** in terms of experimental, calculated and difference traces (blue, red and grey, respectively). The green markers at the bottom indicate the positions of the Bragg reflections.

Supporting Information

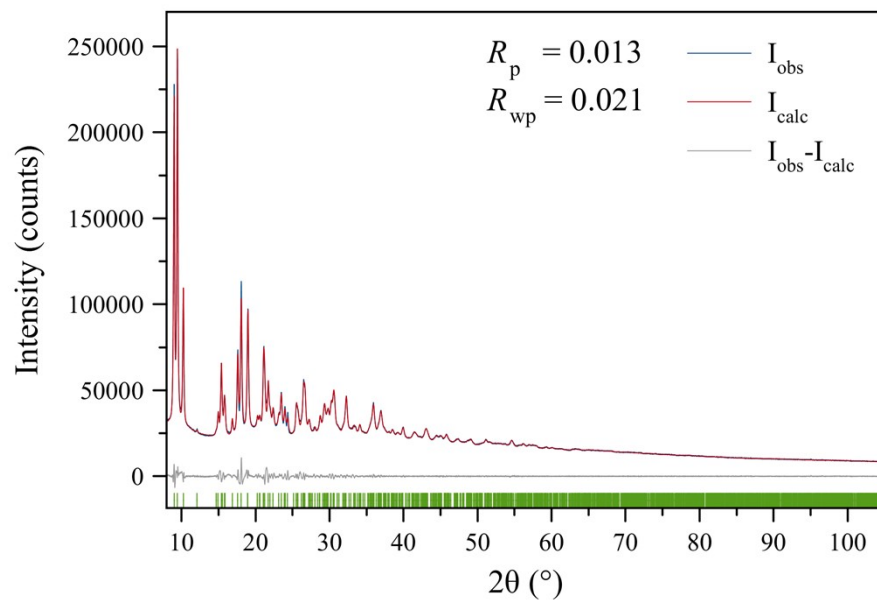
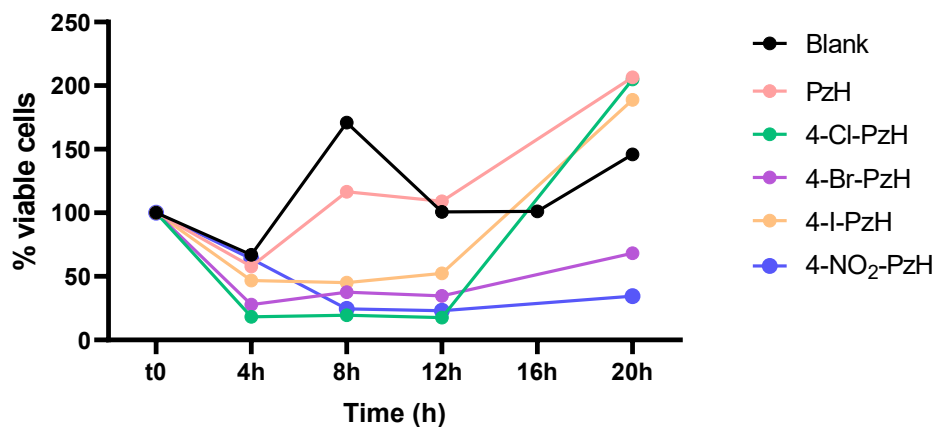


Figure S5. Graphical result of the whole powder pattern refinement carried out with the Le Bail approach on the PXRD pattern of **5** in terms of experimental, calculated and difference traces (blue, red and grey, respectively). The green markers at the bottom indicate the positions of the Bragg reflections.

Supporting Information

Escherichia coli



Staphylococcus aureus

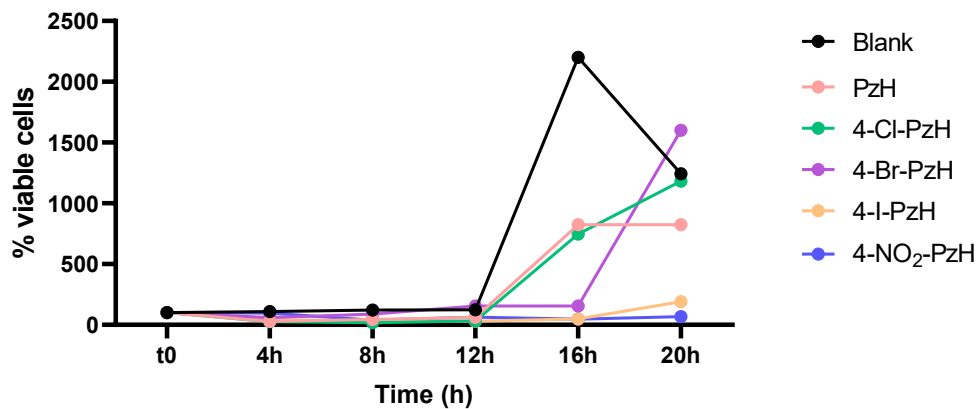


Figure S6. Antibacterial activity of the pyrazole ligands against *E. coli* (up), *S. aureus* (down).